Available online at www.sciencedirect.com

ScienceDirect

Journal of Ocean Engineering and Science 1 (2016) 66–76

www.elsevier.com/locate/joes

Nearshore regional behavior of lightning interaction with wind turbines

Gilbert A. Malinga, John M. Niedzwecki*

Zachary Department of Civil Engineering, Texas A&M University, College Station, TX, USA

Received 29 January 2015; received in revised form 27 April 2015; accepted 13 May 2015
Available online 29 January 2016

Abstract

The severity of lightning strikes on offshore wind turbines built along coastal and nearshore regions can pose safety concerns that are often overlooked. In this research study the behavior of electrical discharges for wind turbines that might be located in the nearshore regions along the East Coast of China and Sea of Japan were characterized using a physics-based model that accounted for a total of eleven different geometrical and lightning parameters. Utilizing the electrical potential field predicted using this model it was then possible to estimate the frequency of lightning strikes and the distribution of electrical loads utilizing established semi-empirical relationships and available data. The total number of annual lightning strikes on an offshore wind turbine was found to vary with hub elevation, extent of cloud cover, season and geographical location. The annual lightning strike rate on a wind turbine along the nearshore region on the Sea of Japan during the winter season was shown to be moderately larger compared to the lightning strike frequency on a turbine structure on the East Coast of China. Short duration electrical discharges, represented using marginal probability functions, were found to vary with season and geographical location, exhibiting trends consistent with the distribution of the electrical peak current. It was demonstrated that electrical discharges of moderately long duration typically occur in the winter months on the East Coast of China and the summer season along the Sea of Japan. In contrast, severe electrical discharges are typical of summer thunderstorms on the East Coast of China and winter frontal storm systems along the West Coast of Japan. The electrical charge and specific energy dissipated during lightning discharges on an offshore wind turbine was found to vary stochastically, with severe electrical discharges corresponding to large electrical currents of long duration.

Keywords: Nearshore wind turbines; Physics based model; Lightning strikes; Electrical current; Strike frequency; Electrical charge.

1. Introduction

Many of the existing offshore wind farms in China and Japan are located in the nearshore region around the East China Sea and Sea of Japan. The proximity of large energy demand centers, driven by massive industrial activity and high domestic consumption, has spurred development of offshore wind energy in these regions. Further, the availability of space for expansion and strong winds offshore provide additional incentives for wind energy developers. A majority of the offshore energy projects in China are located in the intertidal areas of the East China Sea where the average water depths range from 1.0 m to 18 m, making it practical for shallow water foundations such as monopile, gravity based and jacket structures. In contrast, the existing wind farms in Japan are located both along the coast and offshore. The offshore wind turbines along the coast are built on monopile and gravity base foundations in water depths of up to 20 m. The current offshore demonstration projects are located in water depths ranging from 80 m to 150 m. Such experimental projects include Fukushima on the East Coast of Japan, Goto in Nagasaki region and Kabashima Island, where 2 MW and 7 MW floating wind turbines on spar and semi-submersible platforms are undergoing testing [1,2]. Some information on typical offshore wind turbines available in China and Japan is noted in Table 1. The severity of electrical discharges on offshore wind turbines along the East Coast of China and offshore Japan can pose safety concerns. The characteristics of these electrical discharges are anticipated to vary seasonally and geographically as demonstrated in the next section.

* Corresponding author.
E-mail address: j-niedzwecki@civil.tamu.edu (J.M. Niedzwecki).

http://dx.doi.org/10.1016/j.joes.2015.12.004

Table 1
Some offshore wind turbines available in China and Japan.

Country	Company	Blade diameter (m)	Hub elevation (m)	Rated power (MW)
China	China Creative	71–126	65–85	1.5–5.0
	Goldwind	70–109	65–90	1.5–2.5
	Mingyang	77–108	65–100	1.5–3.0
	Shanghai Electric	87–122	65–100	2.0–3.6
	Sinovel	90–113	65–110	1.5–6.0
Denmark	Vestas	80–164	60–140	2.0–8.0
Germany	Siemens	120–154	Site specific	3.0–6.0
Japan	Hitachi	80	60	2.0
	Japan Steel Works	83	65	2.0
	Mitsubishi	92–165	60–105	2.4–7.0

2. Regional lightning characteristics

2.1. Mainland China and adjacent coastal regions

The China Sea is characterized by thunderstorm systems that occur both in the summer and winter months, with peak lightning activity coinciding with the warm season. The behavior of lightning along the coast of China has been well documented. Chen et al. [3] investigated the characteristics of electrical discharges in Guang-Dong Province using field data. The authors found a weak correlation between ground flash density and thunderstorm days. A semi-empirical relationship between ground flash density and thunderstorm days was found to be non-linear.

A strong correlation was found between lightning triggered faults on tall structures and ground flash density. Ming et al. [4] studied the distribution of ground flash density on Mainland China and surrounding regions using satellite imagery. The flash density was shown to vary spatially, with regions of high maxima coinciding with mountainous and coastal locations, especially along the China Sea.

In contrast, low ground flash densities characterize the arid regions of western China. The trends in the ground flash density are consistent with the distribution of the annual precipitation driven by mainly mesoscale convective systems. In another study, Guo-jun et al. [5] investigated the characteristics of lightning in Guangzhou Province using field measurements collected over a 10-year period. The variation in the annual ground flash density was seasonal with peak values of approximately 23 flashes per square kilometer observed in the central region where the terrain is hilly. The mean monthly peak current, which varies approximately from 35 to 95 kA, had moderately large values in the winter months. Further, the number of thunderstorm days was illustrated to vary annually and spatially, with peak values exceeding 95 storm days. In addition, the study demonstrated a strong correlation between lightning activity and weather related damage on engineered structures. Mingyi et al. [6] investigated the distribution of ground flash density and electrical current in Jiangsu Province. The annual ground flash density, which was shown to vary spatially, ranged from 2.4 to 3.6 flashes per square kilometer. The regions of high flash density were shown be located along hilly terrain and around large water masses where convective mesoscale thunderstorm systems are prevalent. Further, lightning of negative polarity was shown to be predominant while positive lightning accounted for only approximately 5% of the lightning strikes. The electrical current, which follows a known semi-empirical function, varied from 20 to 40 kA.

Feng et al. [7] analyzed the behavior of cloud to ground lightning in Fujian region using field measurements. The results show that negative lightning is predominant during the summer season while positive electrical discharges occur mainly in the winter months. The total annual ground flash density was found to vary geographically, from approximately 0.5–9.0 flashes per square kilometer, and the region of high density occurs along the coast. The magnitude of the median electrical current was shown to vary spatially, with a range of 1–70 kA, and the maximum-recorded peak current exceeded 150 kA. The distribution of the lightning parameters was shown to be a function of topography, with severe lightning activity being prevalent along mountainous and coastal regions.

2.2. Coastal and offshore Japan

The severe lightning activity in the Sea of Japan, which occurs mainly in the winter season, is driven by cold frontal storm systems. The summer season along the coast of the Sea of Japan is characterized by mild lightning activity attributed to warm thunderstorm systems. The behavior of lightning along the coast of Sea of Japan has been well documented in several studies. Miyake et al. [8] investigated characteristics of lightning along the coast of the Sea of Japan. Statistical analysis of measured lightning data was conducted to illustrate the distribution of the electrical parameters. The electrical peak current, which ranged from 2 to 100 kA and follows a log normal distribution, comprised of both short and long duration discharges of different polarities. Further, the lightning parameters showed both seasonal and spatial variation, with positive discharges being predominant in the winter months. The duration of the positive electrical current was observed to be longer compared to negative discharges, thus posing the potential to cause large damage to tall structures because of the large quantity of electrical energy dissipated.

Shindo and Yokoyama [9], in a separate study, investigated the relationship between ground flash density and number of storm days in Japan using lightning field data. The study shows that lightning activity on mainland Japan peaks in the summer while electrical discharges along the coast of the Sea of Japan are highest during the winter season. The relationship between ground flash density and thunderstorm days shows a temporal and spatial variation consistent with the reported lightning activity. A semi-empirical relationship correlating ground flash density to thunderstorm days developed by the authors was shown to be inconsistent and varied annually. Therefore, the prediction of thunderstorm days using ground flash density data in Japan may be subject to the limitation of annual variability. Saito et al. [10] investigated the seasonal variation of extreme lightning discharges using data from the Japanese Lightning Detection Network. The elevation of the center of the cloud electrical charge, which varies monthly, was utilized to delimit seasonal boundaries. The results show that the summer season is characterized by high cloud charge centers while those in the winter months are fairly low. Further, the intensity of the negative discharges observed in the summer period was higher than the positive lightning discharges observed in the same time frame. In contrast, positive lightning discharges were more predominant compared to negative lightning in the spring, autumn and winter seasons.

The prevalence of upward lightning, that can be destructive to wind turbines along the coast of the Sea of Japan, was anticipated to be a function of ground flash density and elevation of the cloud charge centers. Shindo et al. [11] investigated the characteristics of cloud to ground lightning in Japan using field measurements. The study showed that the ground flash density in the summer months was an order of magnitude higher than that observed during the winter season. The lightning risk maps developed by the authors show that summer lightning is prevalent on the mainland while the activity in the winter months is concentrated along the coastal areas along the Sea of Japan. The distribution in the electrical current indicated that severe lightning discharges occur in the winter season. Further, monthly variations in the mean peak current were reported, with positive electrical discharges showing large values compared to negative lightning.

2.3. *Lightning interaction with coastal and offshore elevated structures*

The study of lightning strikes to tall structures along coastal and offshore regions is fairly well documented. Miyake et al. [12] investigated lightning interaction with tall structures on the coast of the Sea of Japan using field measurements. The average annual lightning strike frequency on structures with elevations ranging from 80 m to 200 m was reported to vary from 8.5 to 26.3 strikes. Further, lightning discharges to the elevated structures was shown to increase with height of the structure with winter lightning showing a higher intensity compared to electrical discharges observed in the summer. In addition, simultaneous lightning attachment on multiple structures was observed on several occasions. Upward leader behavior, wind direction and thundercloud movement were shown to play a role in lightning attachment on the structures. Wang et al. [13] characterized the behavior of upward leaders incepted from a wind turbine and an adjacent tower using field measurements. The changes in the ambient electric field were used to classify upward lightning on the structures into two categories as self-triggered and downward leader initiated discharges. It was noted that some of the incepted upward leaders did not propagate over long distances due to a weak electric field. The inability to control the impact of the different environmental parameters on lightning behavior in field experiments can be a limitation. Thus, the effect of cloud cover and leader properties on the behavior of incepted upward leaders was not adequately captured. In light of these limitations, an approach based on predictive modeling of upward leader behavior is highly desirable.

In a separate study, Asakawa et al. [14] developed an experimental device to measure lightning discharges on wind turbines built on the northern coast of the Sea of Japan. The experimental study was supplemented with photographic field measurements of upward leader properties. The results showed that a majority of the electrical discharges on the wind turbines were of negative polarity, with 5% of the lightning discharges being positive. Both short and long duration electrical discharges were recorded and the peak current was shown to range from 0.2 to 44.4 kA. The electrical charge dissipated during the lightning discharges on the wind turbines was highly variable and the maximum value recorded was close to 400 C. Ishii et al. [15] investigated the frequency of winter lightning strikes on tall structures on the coast of Japan. The lightning strike frequency was shown to be a function of height of the structure, season of the year and geographical location. Subsequently, the risk of lightning on the tall structures was evaluated using the information derived from the lightning strike rate and distribution of electrical current. The risk of lightning on the tall structures varied temporally and spatially, showing trends consistent with the distribution of the measured electrical parameters. The structures built on the Pacific Coast and mainland Japan experience the highest lightning risk in the summer months. In contrast, the severity of lightning discharges on the structures on coast of the Sea of Japan is greatest in the winter season when upward lightning is predominant and the magnitude of the mean electrical current is largest. Despite the strength of the semi-empirical approach adapted, the study faces the limitation of being unable to account for the effect of multiple environmental parameters such as cloud cover and leader properties on lightning risk on the elevated structures.

Fujil et al. [16] characterized the behavior of winter lightning on wind turbines on the West Coast of Japan. The frequency of lightning strikes on the wind turbines was correlated to elevation of the cloud charge center using field data. The number of lightning strikes on the wind turbines was shown to increase for elevations of the cloud charge center closer to the ground surface, typically taken to be less than 1000 m above the ground level. On the other hand, increase

in the elevation of cloud charge center above 2500 m led to a decrease in the lightning strike rate. Further, the type of storm systems experienced along the West Coast of Japan were shown to have an impact on the distribution of the ground flash density, leader peak current and subsequently the frequency of lightning strikes on the wind turbines. In a follow up study, Ishii et al. [17] investigated the lightning strike behavior around wind turbines in Fukushima on the Pacific coast. The lightning strike rate on the wind turbines was shown to be higher in the winter months compared to the summer, despite the high ground flash density observed during the warm season. The annual lightning strike rate on the wind turbines in Fukushima was shown be an order of magnitude lower compared to the estimates developed for structures of the same elevation built on the coast of the Sea of Japan. Further, a field study on lightning attachment behavior on the turbine blades shows that lightning attachment is function of turbine blade angle for both stationary and moving blades. Lightning parameters such as the extent of cloud cover and downward leader properties are anticipated to affect the development of upward leaders and subsequently lightning attachment on the wind turbine. In addition, it is anticipated that the inherent variation in thunderstorm days, ground flash density and electrical current leads to a stochastic variation in the lightning strike rate on an offshore wind turbine. However, the approach adapted by the authors fails to account for the role of environmental parameters on leader behavior and the probabilistic nature of electrical discharges.

Thus, there remains a need to characterize the role of these environmental parameters and their effect on lightning attachment on an offshore wind turbine. This research study provides an alternative approach of characterizing lightning interaction with an offshore wind turbine. The probabilistic approach adapted here accounts for the stochastic nature of the various lightning parameters and the resulting electrical discharges on an offshore wind turbine operating under varying conditions.

3. Methodology

3.1. *Lightning strike frequency*

Lightning strikes to offshore wind turbines can be characterized as downward and upward initiated strikes based on the mode of leader inception. Downward lightning takes place when a stepped leader propagates from the thundercloud towards the ground surface leading to the intensification of the near field gradient around the wind turbine leading to the inception of upward propagating leaders from the structure providing probable attachment points on the structure. Upward lightning can also be initiated from the periphery of the wind turbine, in absence of the downward leader, when the near field gradient induced by the thundercloud exceeds a designated critical threshold. The development of lightning leaders and their attachment on an offshore wind turbine is demonstrated in Fig. 1. The numerically evaluated potential field around the region swept out by the turbine blades provides the basis for determining the lightning striking rate as a function of turbine hub elevation, blade diameter, cloud cover and leader properties. The striking distance, defined as the distance between the downward leader tip and extreme extent of turbine blade at the instant an upward leader is incepted from the structure, determines the extent of the lightning collection area around the structure. The number of downward lightning strikes to an offshore wind turbine can be determined as a function of ground flash density, lightning collection area and electrical current using a relationship given in the Appendix. In addition, the frequency of upward lightning strikes on the offshore wind turbine is determined as a function of thunderstorm days and upward leader properties as shown in the Appendix. The properties of the incepted upward leader, determined by the near field gradient of the electrical potential around the structure, are evaluated using the inception model described in Becerra et al. [18].

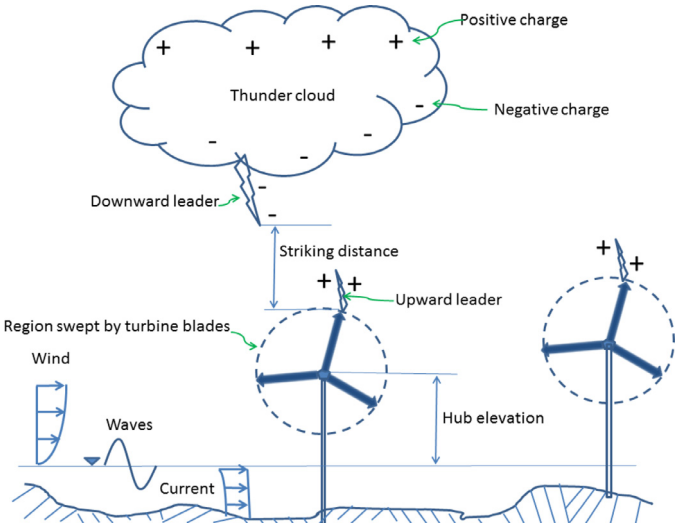

Fig. 1. Schematic illustrating the interaction between lightning and an offshore wind turbine.

3.2. *Electrical discharges on offshore wind turbines*

The total electrical charge dissipated during a lightning discharge on an offshore wind turbine occurs can be separated into two different phases, classified as the short stroke and long stroke processes. The short stroke process involves the impulsive transfer of electrical charge immediately after lightning attachment on the structure. In contrast, the long stroke process, which occurs after at the short impulsive loading, results in dissipation of electrical energy through the structure over a prolonged period, typically greater than 10 ms. The impulsive loads dissipated during the short process are a concern for electronic devices attached on the wind turbine. In contrast, the distributed loads that occur during the long process can affect the material properties of the turbine and in extreme cases can lead to ignition of fire on the structure. Semi-empirical relationships for evaluating the electrical charge dissipated during both the short and long stroke

Table 2
A summary of particulars used in the numerical simulation.

h_e (m)	H (km)	L_D (km)	ϑ (deg.)	I_{peak} (kA)	N_g (flashes per square kilometer per year)	S_D (days)
60–150	1–2	0.4–1.6	60–90	0.5–120	0.05–12	5–160

processes are given in the Appendix. The distribution of the electrical charge and energy dissipated during lightning strikes on an offshore wind turbine shows high variability depending on seasonal, environmental and geographic factors. Therefore, probability density functions are used to characterize the behavior of these electrical discharges. The short stroke electrical charge and energy are represented using marginal probability density functions while the long stroke discharges are represented using both marginal and joint probability functions.

3.3. *Characterization of geometrical and lightning parameters*

The effect of geometry and lightning parameters on the frequency of lightning strikes and distribution of electrical discharges on offshore wind turbines along the East Coast of China and Sea of Japan was investigated. The range of the key design parameters for the study of lightning interaction with an offshore wind turbine is illustrated in Table 2. The hub elevation, h_e of the wind turbine, ranging from 60 m to 150 m, was selected to cover the range of elevations of offshore wind turbines along the East Coast of China and Sea of Japan. The blade diameter of the wind turbine was taken as 90 m. The mean elevation of the thundercloud, H along the East Coast of China was taken as 2000 m, a value consistent with field observations in [19]. The average thundercloud elevation along the nearshore region of the Sea of Japan was selected in conformity with field observations, with a mean elevation of 2000 m in the summer season and 1000 m in the winter months. The length of the stepped leader, L_D assumed to propagate vertically downward, ranges from 430 m to 1600 m. The extent of the cloud cover ϑ was selected to reproduce near field gradients of the electrical potential capable of incepting upward leaders from the periphery of the wind turbine. The magnitude of the electrical potential field at the cloud base was taken as 200 MV, a value consistent with field measurements.

The electrical peak current, I_{peak}, and duration of the electrical discharges on an offshore wind turbine were generated randomly to be consistent with the range of reported lightning discharges on tall structures along the East Coast of China and offshore Japan [5,7,8]. The time frame of the short duration electrical discharges was taken as 1.0 ms. The period of the long duration electrical discharges was assumed to range from 10 to 40 ms. The magnitude of the electrical current in the long duration electrical discharges I_{lpeak} was selected randomly to range from 30 to 75 kA . The randomly generated distributions of the ground flash density, N_g along the East Coast of China and Sea of Japan were assumed to fall within the range of reported data [5,11]. The distribution of the thunderstorm days, S_D on the East Coast of China was generated using a semi-empirical relationship between ground flash density and storm days developed in [3]. The data on thunderstorm days at Akita on the coast of the Sea of Japan was provided by the Japan Meteorological Agency [20].

4. Numerical examples

4.1. *Lightning strike frequency on offshore wind turbines*

The frequency of downward lightning strikes on an offshore wind turbine was evaluated as a function electrical peak current, ground flash density, hub elevation and cloud cover extent. The distributions of the electrical peak current along the East Coast of China and Sea of Japan are illustrated in Fig. 2. The annual distribution of the electrical current along the East Coast of China follows a Gamma distribution with a long upper tail. The electrical current on the coast of the Sea of Japan is approximately Gaussian and exhibits seasonal behavior. The change in season from summer to winter is accompanied by a rightward shift in the distribution of the electrical peak current as shown in Fig. 2b due to the severe electrical discharges that occur in the winter months. The annual ground flash density along the East Coast of China follows a Gaussian distribution as illustrated in Fig. 2c. The coast of the Sea of Japan is characterized by ground flash densities that are seasonally distributed with summer lightning showing values that are an order of magnitude higher than those observed in the winter months as illustrated in Fig. 2d. The annual frequency of downward lightning strikes on an offshore wind turbine built along the East Coast of China and Sea of Japan is shown in Fig. 3. The distributions of the downward lightning strikes on the offshore wind turbine follow trends consistent with the variation in the ground flash density. The estimated number of downward lightning strikes on an offshore wind turbine on the East Coast of China is slightly larger than the seasonal strike rate for structures on the Sea of Japan. Further, the frequency of downward lightning on offshore wind turbines in both the East Coast of China and Sea of Japan did not show much variation with increase in turbine hub elevation.

The upward lightning strike rate on the offshore wind turbine was evaluated as a function of thunderstorm days, turbine hub elevation and cloud cover extent. The distribution of thunderstorm days on the East Coast of China and Sea of Japan is shown in Fig. 4. The annual thunderstorm days on the coast of China closely follow a Gaussian distribution with the peak coinciding with the summer season. On the other hand, the storm days along the coast of the Sea of Japan

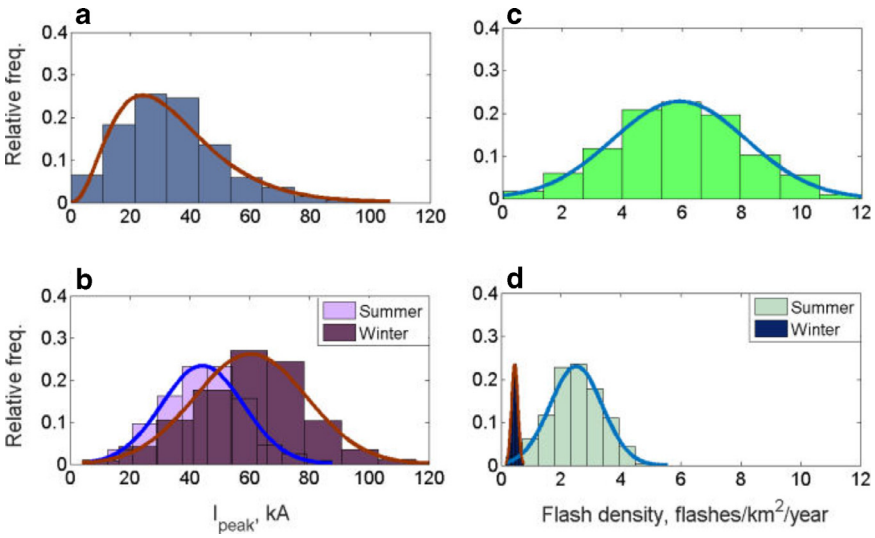

Fig. 2. (a) Distribution of lightning peak current on the East Coast of China, (b) seasonal distribution of electrical peak current on the Sea of Japan, (c) ground flash on the East Coast of China and (d) seasonal distribution of ground flash density along the coast of the Sea of Japan.

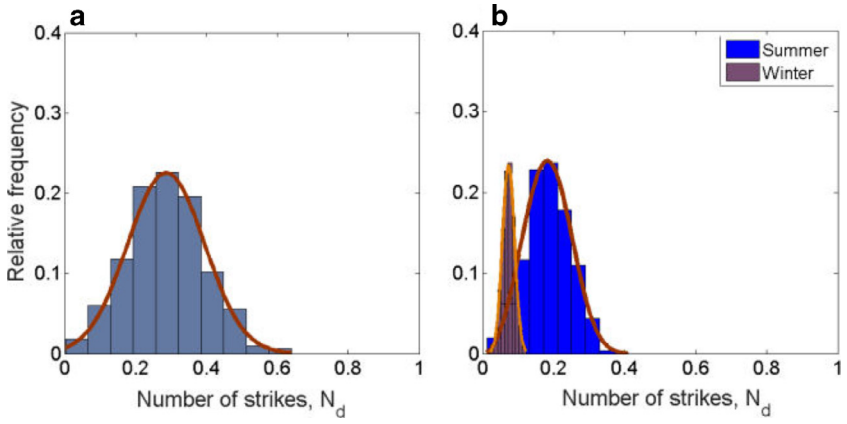

Fig. 3. Distribution of predicted downward lightning strikes on an offshore wind turbine at a hub elevation of 60 m built along (a) East Coast of China and (b) Sea of Japan.

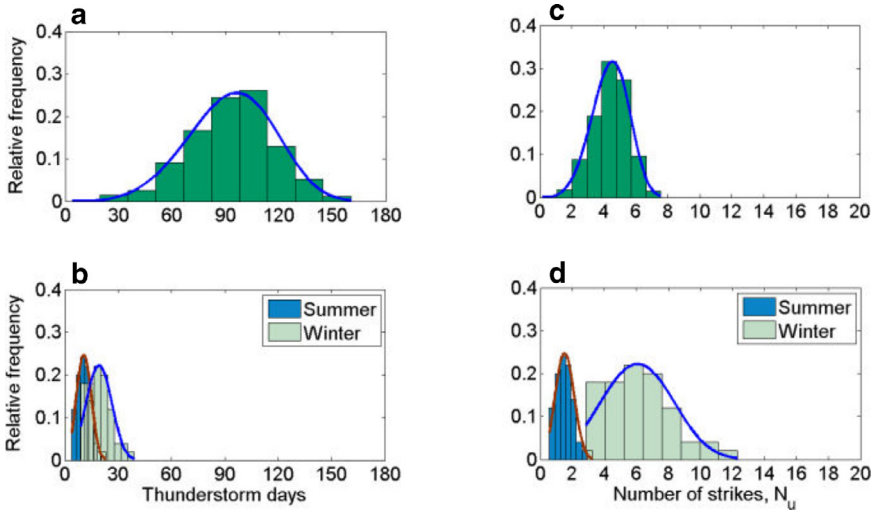

Fig. 4. Distribution of thunderstorm days along (a) East Coast of China and (b) coast of the Sea of Japan. The distribution of predicted upward lightning strikes on an offshore wind turbine at a hub elevation of 60 m placed along (c) East Coast of China and (d) coast of the Sea of Japan. The extent of cloud cover was taken as 90°.

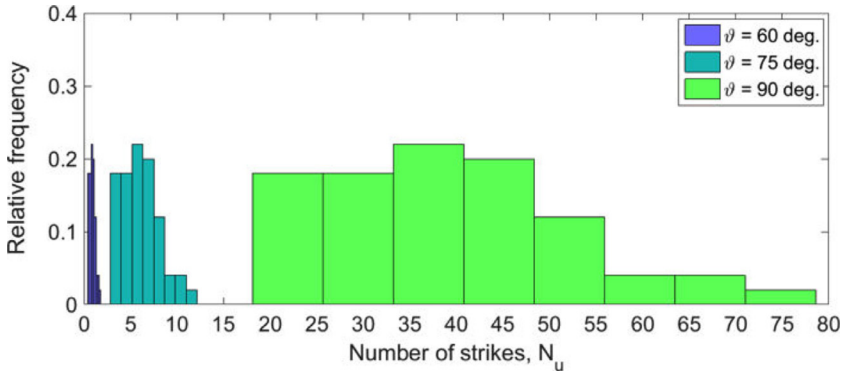

Fig. 5. Distribution of predicted upward lightning strikes on an offshore wind turbine at a hub elevation of 150 m in the winter season as a function of cloud cover extent for structures built along the coast of the Sea of Japan.

Table 3
Summary of predicted upward lightning strike rate for offshore wind turbines built along the East Coast of China and Sea of Japan. The extent of cloud cover was taken as 90°.

h_e (m)	East Coast of China		Sea of Japan, summer		Sea of Japan, Winter	
	μ	σ	μ	σ	μ	σ
60	4.41	1.15	1.54	0.54	6.13	2.07
120	5.57	1.45	1.95	0.68	23.20	7.83
150	6.61	1.72	2.31	0.81	39.05	13.17

are log normally distributed with the winter season showing slightly higher activity than the summer. The frequency of upward lightning strikes on an offshore wind turbine on the East Coast of China and Sea of Japan follow trends consistent with the distribution of thunderstorm days as illustrated in Fig. 4c and d, respectively. The lightning strike rate on an offshore wind turbine on the Sea of Japan is moderately higher in the winter months than in the summer season due to the lower mean thundercloud elevation observed during the cold season. Overall, the lightning activity on the Sea of Japan is more severe compared to the East Coast of China, posing a higher risk of lightning on wind turbines built offshore Japan.

The effect of varying the extent of cloud cover on the frequency of upward lightning on an offshore wind turbine along the coast of the Sea of Japan is illustrated in Fig. 5. Increasing the size of cloud cover leads to a rightward shift in the strike rate distribution. This behavior is attributed to the increase in the near field gradient, around the wind turbine, with increase in cloud size leading to an increased likelihood of incepting upward leaders, which propagate over longer distances, and thereby increasing the probability of lightning attachment on structure.

The effect of turbine hub elevation on the upward strike rate is demonstrated in Table 3. An increase in hub elevation is accompanied by a moderate increase in the number of upward lightning strikes on the offshore wind turbine. The upward strike rate data is log normally distributed with a slight positive skew and shows increased spread as the hub elevation moves higher. This can be attributed to the increase in the near field gradient around the wind turbine as the hub elevation moves higher, leading to the inception and growth of energetic upward propagating leaders.

4.2. *Short and long duration electrical discharges*

The characteristics of short duration electrical loads imposed on an offshore wind turbine are illustrated in Fig. 6. The probability distributions of the electrical charge and energy dissipated during a short stroke discharge on an offshore wind turbine along the coast of the East Coast of China are given in Fig. 6a and b, respectively. The trends in the electrical charge are consistent with the distribution of the electrical peak current, with the mean value coinciding with the average peak current. The specific energy is exponentially distributed with a long upper tail. On the other hand, the lightning loads on an offshore wind turbine on the coast of the Sea of Japan are seasonally distributed as shown in Fig. 6c and d. The change in season from summer to winter is accompanied by a rightward shift in the probability distribution of both the electrical charge and specific energy dissipated, indicating behavior consistent with the seasonal distribution of the electrical peak current. The distribution of the electrical charge is close to Gaussian while the specific energy is log normally distributed with a long upper tail. The estimates of the electrical charge and energy dissipated fall within the range of reported data in [8]. These impulse electrical loads can cause problems for electronic devices placed on an offshore wind turbine and therefore should be adequately dissipated in order to prevent damage to the structure.

The bivariate distribution between the long period electrical loads imposed on the wind turbine and duration of the electrical discharge are illustrated in Fig. 7. The behavior of the electrical current and corresponding duration of the electrical waveform is demonstrated in Fig. 7a. Moderate duration peak currents are characteristic of electrical discharges

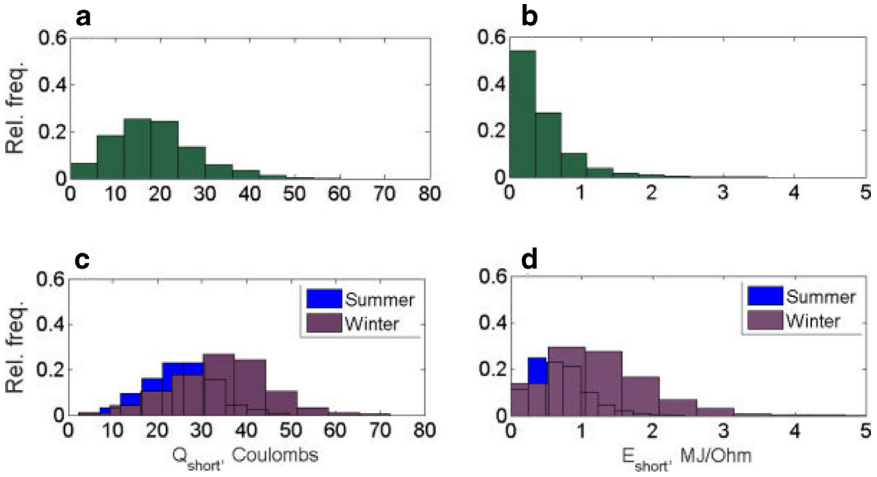

Fig. 6. Distribution of short stroke (a) electrical charge and (b) specific energy discharged on an offshore wind turbine on the East Coast of China, (c) seasonal distribution of long duration electrical charge and (d) long duration specific energy dissipated on a wind turbine along the coast of the Sea of Japan.

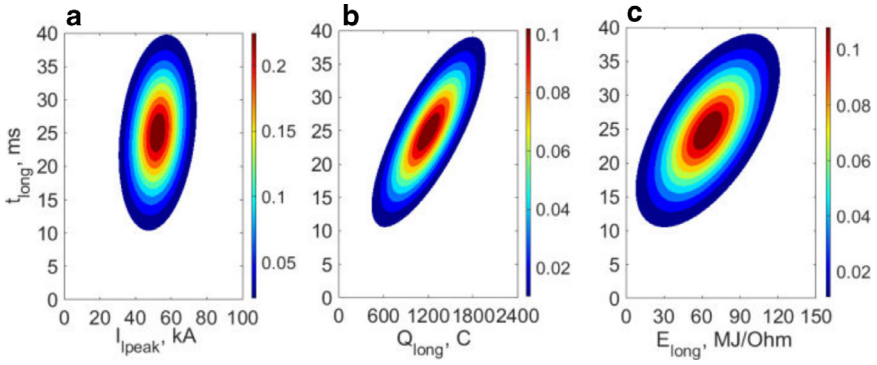

Fig. 7. Normalized joint probability distribution between duration of lightning discharge and (a) electrical current, (b) electrical charge and (c) specific energy dissipated on an offshore wind turbine built along the East Coast of China and Sea of Japan.

Table 4
Summary of predicted electrical discharge data on offshore wind turbines along the East Coast of China and Sea of Japan.

t_{long} (ms)	Electrical charge, Q_{long} (C)		Specific energy, E_{long} (MJ/Ohm)	
	μ	σ	μ	σ
10	412.14	92.73	20.96	8.57
15	618.21	139.10	31.43	12.86
30	1236.40	278.19	62.87	25.72

observed in mild convective storm systems along the East Coast of China in the winter months and coastal regions along the Sea of Japan in the summer season. In contrast, the severe electrical discharges are typical of warm convective storms on the coast of China and cold frontal thunderstorm systems along the West Coast of Japan. These large electrical discharges can be highly destructive to tall structures as reported in [8,14]. The resulting electrical charge and specific energy dissipated are illustrated in Fig. 7b and c, respectively. The electrical charge is characterized by an asymmetric bivariate Gaussian distribution with severe discharges corresponding to large peak currents of long duration typical of summer lightning on the East Coast of China and winter lightning along regions adjacent to the Sea of Japan. The distribution of the specific energy dissipated is also asymmetrically distributed, with the large electrical loads posing problems for offshore wind turbines that cannot adequately dissipate the excess energy. The estimates of the dissipated electrical loads fall within the range of reported data for tall structures built along the coast of the Sea of Japan as shown in [8]. The effect of increasing duration of the lightning discharge on electrical loads dissipated on an offshore wind turbine is demonstrated in Table 4. The mean electrical charge and specific energy dissipated increase with the duration of the lightning discharge. Further, the spread in the data increases with the duration of electrical discharge and energy dissipated. The electrical charge is log normally distributed with a slight skew to the left. In contrast, the specific energy dissipated follows a

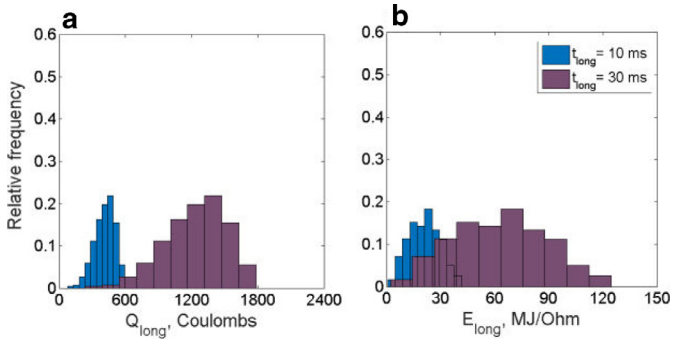

Fig. 8. Marginal distribution of long stroke (a) electrical charge and (b) specific energy dissipated on an offshore wind turbine as a function of duration of the electrical discharge for structures built along the East Coast of China and Sea of Japan.

Gaussian distribution with little skew in the data. Lightning discharges of longer duration lead to a rightward shift in the distribution of the electrical charge and energy dissipated as illustrated in Fig. 8. The estimates of the long duration electrical charge and energy dissipated on an offshore wind turbine clearly exceed the IEC design thresholds [21]. This reinforces the need to investigate the impact of extreme electrical loads on wind turbines built in nearshore regions with severe lightning behavior.

5. Summary and conclusions

The behavior of electrical discharges on wind turbines placed in the nearshore region along the East Coast of China and Sea of Japan was investigated using a physics based approach that takes into account the effect of eleven different parameters associated with actual geometrical and lightning parameters. The geometrical parameters include blade diameter, turbine hub elevation, cloud base elevation, extent of cloud cover, length of downward leader and its propagation angle. The lightning parameters include cloud potential field, electrical peak current, ground flash density, thunderstorm days and duration of the electrical discharge. The numerically evaluated electrical potential field around the wind turbine was then used to characterize the frequency of lightning strikes on an offshore wind turbine as a function of these model parameters. Further, the distribution of electrical loads imposed on a wind turbine was evaluated using randomly generated data, consistent with field observations along the nearshore region on East Coast of China and the Sea of Japan.

The frequency of downward lightning strikes on an offshore wind turbine was shown to vary with geographical location and season. The downward lightning strike rate on an offshore wind turbine along the East Coast of China was found to be slightly larger compared to the seasonal strike frequency on turbine structures along the coast of the Sea of Japan. The hub elevation of the wind turbine had minimal impact on the downward lightning strike frequency. The number of upward lightning strikes on an offshore wind turbine was found to vary geographically and seasonally, behavior consistent with the distribution of the thunderstorm days. The upward lightning strike rate on a wind turbine along the coast of the Sea of Japan is moderately higher in the winter months than in the summer season due to the lower mean thundercloud elevation observed during in the winter season. Further, the upward lightning activity on the Sea of Japan was demonstrated to be more severe compared to the East Coast of China, posing a higher risk of electrical discharges on structures built in the nearshore and offshore Japan. The effect of varying the extent of the cloud cover on the upward lightning strike rate on an offshore wind turbine resulted in a rightward shift in the lightning strike data. The increase in the lightning strike rate with cloud cover extent was attributed to the magnification of the near field gradient of the electrical potential, in the vicinity of the wind turbine, with increase in cloud size leading to an increased likelihood for upward leader inception. Further, the upward strike frequency was found to increase with the hub elevation of the wind turbine.

The impulse electrical loads imposed on an offshore wind turbine represented using probability functions were demonstrated to vary with geographical location and season. The trends in the electrical charge were shown to be consistent with the distribution of the lightning peak currents, with the mean value coinciding with the average peak current. The specific energy was illustrated to follow a non-Gaussian distribution with a long upper tail. Short duration electrical loads can cause problems for electronic devices placed on an offshore wind turbine and therefore should be adequately dissipated in order to prevent damage to the structure. The magnitude and duration of the distributed electrical discharges imposed on an offshore wind turbine were represented using bivariate probability functions. The electrical currents of moderate duration are characteristic of lightning observed along the East Coast of China during the cold season and on the West Coast of Japan in the summer months. In contrast, severe electrical discharges are typical of warm convective storms on the East Coast of China and cold frontal thunderstorm systems along the nearshore region on the West Coast of Japan. The long duration electrical charge and specific energy dissipated were illustrated using asymmetric bivariate distributions. The severe electrical discharges correspond to large peak currents of long duration and are typical of summer lightning on the East Coast of China and winter lightning on the West Coast of Japan. The numerical predictions for the long duration electrical charge and energy dissipated on an offshore wind turbine exceed the recommended IEC design thresholds. Based on these findings, additional investigation regarding the impact of extreme electrical loads on wind turbines built in nearshore regions with severe lightning conditions appears warranted.

Acknowledgments

The writers gratefully acknowledge the partial financial support of the Wofford Cain '13 Senior Endowed Chair in Offshore Technology at Texas A&M University during this research study. We also are indebted to Ms. He Yang at Texas

A&M University for her assistance in translating several of the technical publications published in Chinese that were used in this research study.

Appendix. Lightning model

The behavior of lightning discharges on a wind turbine built along the nearshore region along the East Coast of China and Sea of Japan was investigated using a physics based model that takes into account eleven different problem parameters. These include geometrical parameters the blade diameter, hub elevation of wind turbine, cloud base elevation, extent of cloud cover, length of downward leader and its propagation angle, the cloud potential field, electrical peak current, ground flash density, thunderstorm days and duration of the electrical discharge. The numerically evaluated potential field around the wind turbine was validated using exact mathematical solutions. The solution of the electrical potential field provided the basis for determining the frequency of lightning strikes on the offshore turbine. Further, the distribution of electrical loads on the wind turbine was determined using established semi-empirical relationships.

The number of annual negative downward lightning strikes, N_d, to an offshore wind turbine is given by the following form [22]:

$$N_d = N_g \int_{I_{p\min}}^{I_{p\max}} A_c(I_{peak})\ f(I_{peak})\ dI_{peak} \tag{1}$$

where N_g is the ground flash density, A_c is the lightning collection area, $I_{p\,min}$ and $I_{p\,max}$ are the lower and upper bounds of the leader peak current, I_{peak}, respectively, and $f(I_{peak})$ is the probability density function of the leader peak current.

The number of positive upward lightning strikes triggered from an offshore wind turbine in absence of a downward leader, N_u, is given by the following modified expression [22]:

$$N_u = S_D\, f_g\, P(L > L_{th}) \left(\frac{\bar{L}}{h_e}\right) \tag{2}$$

where S_D is the total number of storm days in a year,f_g is a factor that accounts for the effect of geographical location, taken as unity for the East Coast of China and 3 for the nearshore region along the Sea of Japan in order to reproduce strike rates consistent with field observations in [12], $P(L > L_{th})$is the probability of the incepted upward leader length, L, exceeding the threshold length for inception of an upward leader, L_{th}, taken as 2 m, $\bar{L}$ is the mean length of the incepted upward leader and h_e is the hub elevation of the offshore wind turbine. The annual total number of lightning strikes on the offshore wind turbine is the sum of the downward and upward-triggered strikes.

The electrical charge dissipated during a lightning discharge on an offshore wind turbine is evaluated as the integral of the current waveform in the short and long stroke processes, respectively, as shown by the following expression [21]:

$$\begin{aligned} Q_{short} &= \int_0^{t_{short}} I_{short}(t)\ dt \\ Q_{long} &= \int_0^{t_{long}} I_{long}(t)\ dt \end{aligned} \tag{3}$$

where Q_{short} and Q_{long} are the total electrical charge dissipated during short and long stroke processes in Coulombs, respectively, $I_{short}(t)$ is the short stroke current in amperes, $I_{long}(t)$ is the long stroke current in amperes, t_{short} is the duration of the short stroke and t_{long} is the duration of the long stroke in seconds. The short stroke discharges occur immediately after the lightning attachment on an offshore wind turbine and are characterized by pulsed dissipation of electrical energy. In contrast, long duration discharges occur after the pulsed loads and involve discharge of large amounts of electrical energy over a longer time frame.

The specific energy dissipated during an electrical discharge on an offshore wind turbine is given by the following expression [21]:

$$\begin{aligned} E_{short} &= \int_0^{t_{short}} (I_{short}(t))^2\ dt \\ E_{long} &= \int_0^{t_{long}} (I_{long}(t))^2\ dt \end{aligned} \tag{4}$$

where E_{short} and E_{long} are the specific energy dissipated during the short and long stroke processes, respectively.

The short stroke current is represented using a semi-empirical relationship of the form [21]

$$I_{short}(t) = \frac{I_{peak}}{k_f}\left[\frac{\left(\frac{t}{\tau_1}\right)^{10}}{1+\left(\frac{t}{\tau_1}\right)^{10}}\right]\exp\left(-\frac{t}{\tau_2}\right) \tag{5}$$

where I_{peak} is the short stroke peak current in amperes, k_f is the correction factor for the amplitude of the short stroke peak current and is determined from a parametric analysis, t is the time in seconds, τ_1 is the front time constant, representing the ascending portion of the wave form and τ_2 is the tail time constant defining the extent of the decaying portion of the current waveform. The short stroke process was assumed to comprise a single stroke with a duration of 1.0 ms.

The electrical waveform for the long stroke current is represented using a filter function in [23] and modified by Malinga and Niedzwecki [24] as shown by the following expression:

$$\begin{aligned} I_{long}(t) &= I_{lpeak}\left[f_1(t) + f_2(t)\right] \\ f_1(t) &= \left[1+\left(\frac{t_{long}-t}{t_{long}-t_{front}}\right)^{2k_{long}}\right]^{-0.5}, \quad 0 \le t \le t_{front} \\ f_2(t) &= \left[1+\left(\frac{t}{t_{tail}}\right)^{2k_{long}}\right]^{-0.5}, \quad t_{front} < t \le t_{long} \end{aligned} \tag{6}$$

where I_{lpeak} is the long stroke peak current in amperes, $f_1(t)$ and $f_2(t)$ are functions that characterize the shape of the current wave form, k_{long} is a dimensionless shape parameter that controls the gradient of the rising and decaying portions of the wave form, t_{front} is the duration of the rising portion of the current wave form and t_{tail} is the time the current starts to decay. The total duration of the long stroke current was assumed to be randomly distributed and the corresponding duration for the front current and start time for the tail current were taken as 10% and 90% of the total duration, respectively.

References

[1] Maine (2013). Floating offshore wind foundations: Industry consortia and projects in the United States, Europe and Japan. http://www.maine-intl-consulting.com/4.html. (accessed 12.12.14.).

[2] Marubeni (2014). Fukushima recovery/ floating offshore wind farm experimental project. https://www.marubeni.com/project_story/wind. (accessed 12.12.14.).

[3] M.S. Chen, Y. Du, L.M Fan, IEEE Trans. Power Deliv. 19 (3) (2004) 1148–1153.

[4] M. Ming, T. Shanchang, Z. Baoyou, L. Weitao, Sci. China Ser. D: Earth Sci. 45 (2) (2005) 219–229.

[5] L. Guo-jun, X. Jun, C. Jia-hong, T. Xue-fang, G. Shan-qiang, High Volt. Eng. 35 (12) (2009) 2930–2936.

[6] X. Mingyi, W. Zhenhui, F. Rong, Z. Junchi, Z. Qingfeng, J. Nanjing Univ. Inf. Sci. Technol.: Nat. Sci. Ed. 2 (6) (2010) 557–561.

[7] Z. Feng, Z. Jinquan, Z. Yefang, W. Yingbo, J. Nat. Disasters 22 (4) (2013) 213–221.

[8] K. Miyake, T. Suzuki, K. Shinjou, IEEE Trans. Power Deliv. 7 (3) (1992) 1450–1457.

[9] T. Shindo, S. Yokoyama, IEEE Trans. Power Deliv. 13 (4) (1998) 1468–1474.

[10] M. Saito, M. Ishii, M. Matsui, F. Fujil, IEEE Trans. Power Energy 132 (6) (2012) 536–541.

[11] T. Shindo, H. Motoyama, A. Sakai, N. Honma, J. Takami, M. Shimizu, K. Tamura, K. Shinjo, F. Ishikawa, Y. Ueno, M. Ikuta, D. Takahashi, IEEJ Trans. Electr. Electron. Eng. 7 (3) (2012) 251–257.

[12] K. Miyake, T. Suzuki, M. Takashima, M. Takuma, T. Tada, IEEE Trans. Power Deliv. 5 (3) (1990) 1370–1376.

[13] D. Wang, N. Takagi, T. Watanabe, H. Sakurano, M. Hashimoto, Geophys. Res. Lett. 35 (2) (2008).

[14] A. Asakawa, T. Shindo, S. Yokoyama, H. Hyodo, IEEJ Trans. Electr. Electron. Eng. 5 (1) (2010) 14–20.

[15] M. Ishii, M. Saito, F. Fujil, M. Matsui, N. Itamoto, Electr. Eng. Jpn. 170 (1) (2010) 291–297.

[16] F. Fujil, M. Ishii, M. Saito, M. Matsui, Electr. Eng. Jpn. 184 (2) (2013) 973–978.

[17] M. Ishii, M. Saito, D. Natsuno, A. Sugita, in: Proceedings of International Conference on Lightning Protection, Shanghai, China, 2014.

[18] M. Becerra, Cooray V., Z. Hartono, J Electrostat. 65 (2007) 562–570.

[19] Y. Li, R. Yu, X. Zhang, J. Meteorol. Soc. Jpn. 82 (2) (2004) 761–773.

[20] Japan Meteorological Agency (JMA) (2014). Meteorological data. http://www.jma.go.jp/jma/indexe.html. (accessed 11.12.14.).

[21] International Electrotechnical Commission IEC, IEC 61400-24 Standard, Wind Turbines-Part 24: Lightning Protection, IEC Press, Geneva, 2010.

[22] G. Malinga, Niedzwecki, J. Eng. Math. (2015) (on-line).

[23] J. Roberts, T.D. Roberts, J. Geophys. Res.: Oceans 83 (C11) (1978) 5510–5514.

[24] G Malinga, Niedzwecki, J. Ocean Wind Energy 2 (2) (2015) 81–88.